A Decision Support Framework for Resilience-Oriented Cost-Effective Distributed Generation Expansion in Power Systems

Tazim Ridwan Billah Kushal
Student Member, IEEE
The Ohio State University
2015 Neil Ave, Dreese Lab 205
Columbus, OH 43210, USA
kushal.1@osu.edu

Mahesh S. Illindala
Senior Member, IEEE
The Ohio State University
2015 Neil Ave, Dreese Lab 205
Columbus, OH 43210, USA
millindala@ieee.org

***Abstract*—Resilience of electricity grids to rare but severely disruptive events, such as natural disasters, has emerged in recent years as the most important aspect in power system planning. This paper presents a novel approach to enhance the resilience of a system by leveraging the distributed nature of solar photovoltaic (PV) and battery energy storage system (BESS) resources. The proposed decision-making framework uses analytic hierarchy process (AHP) to evaluate different possible allocations of PV and BESS resources for multiple contingencies based on resilience enhancement and cost. The trade-off between cost and resilience is modeled via cost-effectiveness analysis (CEA) that indicates the preferability of each allocation plan. The main contribution of this paper is the development of an adaptable and computationally feasible decision support framework to determine cost-effective configurations of PV arrays and BESSs for mitigating the effects of transmission line outage contingencies. To evaluate the proposed framework, a case study is carried out on the IEEE 33-bus radial distribution system. The results show that the proposed method can offer effective guidance to the planner for making informed decisions about spending resources and achieving cost-effective resilience enhancement.**

***Index Terms*—Decision support systems, distributed generation, power system resilience, renewable energy**

I. Introduction

A. Background and Motivation

Traditional electric power systems are designed to operate during certain contingencies based on the reliability criteria of security and adequacy. These contingencies result from the breakdown of system components, and they have predictable impacts with known failure rates. However, catastrophic events such as natural disasters, which occur rarely but have a large and unpredictable impact, present a challenge to this reliability-based planning of power systems. Recent examples include Hurricanes Harvey and Irma in 2017, two of the costliest storms in the history of the United States. Hurricane Harvey was estimated by the National Oceanic and Atmospheric Administration (NOAA) to have caused $125 billion in total damages and about 220,000 customers to lose power [1]. Several Caribbean islands and the U.S. state of Florida suffered extensive damage from Hurricane Irma, which caused widespread destruction of power lines and almost total loss of electricity in Puerto Rico [2]. In the period 2003-2012, over 50,000 U.S. customers were impacted by 679 power outages due to weather-related events [3]. According to data from the North American Electric Reliability Council (NERC), 933 blackouts were reported between 1984 and 2006, each affecting tens or even hundreds of thousands of customers [4]. Such contingencies require power system resilience to be considered since they cannot be addressed through traditional reliability-oriented planning.

Resilience is a concept distinct from reliability and indicates the ability of a system to deal with low-frequency high-impact events [5]. A resilient system must maintain performance during potentially unprecedented contingencies with uncertain and rapidly varying parameters [6]. Current practices with regard to distribution restoration leave the grid vulnerable to extreme weather events and are therefore not considered sufficiently resilient [7]. Probabilistic fragility modeling by Panteli et al. has shown that adaptation measures are necessary to ensure power system operation during extreme weather, particularly when key parameters such as wind speed are uncertain [8]. A study of the hazardous effects of wind storms in the Northeast U.S. using Sequential Monte Carlo simulations indicated the vulnerability of the grid to outage and the need for system hardening against wind storms [9]. Risk assessment modeling in [10] based on the application of data-mining techniques on historical outage data concluded that the U.S. electricity grid is especially vulnerable to severe wind events such as hurricanes and tornadoes.

B. Literature review

Researchers have proposed various methods of enhancing the resilience of power systems [11]–[18]. One approach is to divide the grid into a number of smaller grids (islands) according to some grouping criteria to minimize load shedding and facilitate load restoration [11], [12]. A hierarchical outage management scheme has been used to design a resilient power distribution system encompassing multiple microgrids with

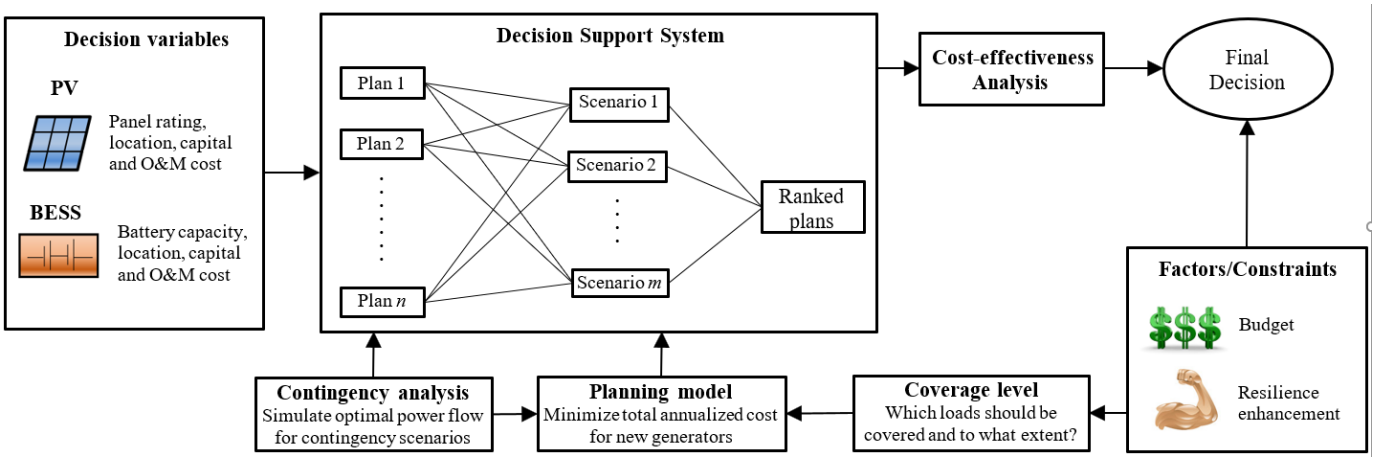

Fig. 1. Overview of the decision support framework.

distributed control [13]. Another method of quantifying and enhancing resilience of a multi-microgrid system based on percolation theory was proposed in [14]. The feeder restoration approach presented in [15] uses distributed energy resources (DERs) to supply the critical loads in a power distribution system when the main grid supply is unavailable. Fang and Sansavini formulated resilience-oriented investment in transmission line expansion and switching devices as a tri-level optimization problem [16]. Replacing sections of a power system with underground natural gas transportation systems has been shown to improve the grid resilience [17]. In [18], a shipboard power system was made more resilient using a strategy of adding power lines based on graph theory.

Recent research has focused on exploiting the potential of locally available generation by using DERs to improve the resilience of the electric grid, especially on the distribution side, which has been shown by past experience as the most vulnerable part of the infrastructure [19]. The same paper proposed additional energy capacity to be added in the form of solar photovoltaic (PV) devices and battery energy storage system (BESS). However, the intermittent nature of PV poses a more challenging problem than dispatchable generation expansion planning due to potential mismatch between power supply and demand. Several methods of optimally sizing PV systems have been proposed [20]–[26]. PV arrays are often combined with other technologies, such as wind power [20]–[23] and biomass [26], since combinations of multiple technologies tends to increase the system reliability [27]. Additionally, PV arrays are coupled with energy storage such as BESS to resolve the problem of intermittent power output [28] and control power injection rate for system stability [29]. Their optimal sizing is generally treated as an optimization problem with a trade-off between cost and system reliability. Multi-objective approaches can include environmental considerations such as reduction of emissions (greenhouse gases and air pollutants) and fuel savings, either directly by maximizing the use of zero-emission sources [26] or indirectly (in grid-connected scenarios) by minimizing power purchases from the utility grid [22].

C. Contribution

Literature concerning the planning of power systems based on PV and other renewable sources has generally focused on minimizing cost and ensuring reliability. Resilience has not been considered as an issue of interest. However, many of the outages reported in [1]–[4] result from damaged transmission lines, which are crucial for the operation of conventional power systems with large generation capacities aggregated at a limited number of nodes. Renewable power generators tend to be distributed throughout the system and require fewer transmission lines [30], thus reducing the number of potential points of failure. This paper aims to enhance the resilience of a power grid by exploiting the distributed nature of PV systems, which have greater sizing and siting flexibility than fossil fuel plants, along with BESSs to resolve the intermittency issue. Since adding more units would increase the resilience but would also cost more, cost-effectiveness analysis (CEA) is used to measure the performance per dollar spent. The major contribution of this paper is a flexible and scalable decision support system for PV system sizing and siting that leverages its distributed nature to achieve higher resilience in a power distribution system. Among its key advantages is the absence of complexities involved in planning for distribution systems, where simplifying assumptions are not justifiable and non-linearities cannot be ignored in optimization. It can incorporate a large number of contingency scenarios without stochastic programming, since they are weighted on the basis of severity rather than probability of occurrence.

D. Paper organization

The proposed framework is organized into the following sections. Section II describes the methodology of simulating contingencies, ranking allocation plans and the decision support tool. Section III explains the planning stage, where PV and BESS resources are optimally allocated for each scenario. Case study of a radial power distribution system using the

proposed framework is presented in Section IV. Section V concludes the paper.

II. Multi-contingency planning

The ability of a power system to supply loads is impaired by a transmission line outage, which prevents power flow through a subset of lines. This can happen because of direct physical damage to the line or tripped circuit breakers due to overloading. Whatever the reason, it often ultimately causes a supply shortfall that results in some unserved load. In this study, the amount of unserved load is used as the measure of resilience.

A. Contingency Analysis

At any time, the state of a power system can be determined by running a power flow model. If the loads are considered dispatchable, this can also show the unserved load. The minimum unserved load under any condition may be determined by solving the cost-minimizing optimal power flow (OPF) problem, with a large cost incurred for any loads shed. Security-constrained OPF (SCOPF) can be used to deal with known contingencies by planning optimal corrective actions after a disruptive event [31]. However, the SCOPF formulation becomes increasingly complex as the pre-specified set of contingencies grows larger. The order of contingency k, which in this study is the number of disabled transmission lines, determines the number of scenarios. For a system with n branches, the number of possible contingencies with k lines disabled is $\binom{n}{k}$. The IEEE 33-bus test system has 32 branches (excluding the normally-open tie lines) and for k = 1, 2, 3 and 4 the number of scenarios is 32, 496, 4960 and 35960 respectively. Since the set of scenarios grows rapidly with the order of the contingency, it may not be computationally feasible to consider all the possible scenarios. Robust programming approaches circumvent this problem by only selecting the worst contingencies using, for instance, a bi-level max-min formulation [32]. But this method has the disadvantage of increasing the cost by considering the worst possible scenario. This paper simulates the operating condition of the power system using conic programming, which offers a convenient way to solve OPF for radial AC systems using convex optimization [33]. The full non-convex optimization problem is reduced to a second-order cone programming (SOCP) problem by relaxing some constraints and eliminating other sinusoidal ones. The AC OPF is run for various contingencies and the results are used in the decision process.

B. Analytic Hierarchy Process

The Analytic Hierarchy Process (AHP) is a numerical framework for complex multiple criteria decision making [34]. It is a flexible decision support tool that can account for both objective realities and subjective experience through pairwise comparison of criteria and alternative options. Relative importance of each criterion with respect to all other criteria is expressed numerically, so that a higher number corresponds to greater importance. Similarly, each option is also compared against all other options under consideration and the relative preference, with respect to each criterion, is expressed as a number. If the number of criteria considered in a decision process is m, then a $m \times m$ pairwise comparison matrix of criterion weights $\mathbf{A}$ can be defined so that the element a_{jk} expresses the importance of the j-th criterion relative to the k-th criterion. With n alternative options being considered, a $n \times n$ pairwise comparison matrix $B^{(i)}$ can be constructed such that the element $b_{jk}^{(i)}$ indicates how preferable the j-th option is to the k-th option, with respect to the i-th criterion.

$$w_j = \frac{\sum_{k=1}^{m} \frac{a_{jk}}{\sum_{l=1}^{m} a_{lk}}}{m} \tag{1}$$

$$s_i^{(j)} = \frac{\sum_{k=1}^{n} \frac{b_{ik}^{(j)}}{\sum_{l=1}^{n} b_{lk}^{(j)}}}{n} \tag{2}$$

The pairwise comparison matrices are used to calculate the m-dimension criteria weight vector $\mathbf{w}$ and the n-dimensional option score vector $\mathbf{s}^j$ by normalization with the column sum and taking the row average, as shown in (1)–(2). The full $n \times m$ option score matrix is $\mathbf{S} = [\mathbf{s}^{(1)}\mathbf{s}^{(2)}...\mathbf{s}^{(m)}]$. As the final output, the AHP method assigns each option an overall score. The global score vector $\mathbf{v}$ gives the score for each option and is calculated as shown below.

$$\mathbf{v} = \mathbf{S}\mathbf{w} \tag{3}$$

The score of an option is a number that indicates its preferability. All n options can be arranged from most desirable to least desirable by arranging them in descending order of scores. In planning generation expansion for multiple contingencies, there is the issue of deciding the best plan for all possible scenarios. In this study, AHP has been used to solve this problem, by considering the contingencies as criteria and the plans as options. Criteria weights are assigned based on the severity of the contingencies, as indicated by the unserved load. Option scores are decided based on the performance of the plans in each scenario, evaluated on the basis of the power supplied and the annual cost. Cost-effectiveness of one option relative to another is calculated using the CEA metric of incremental cost effectiveness ratio (ICER). Since a lower ICER mean higher preferability, the utility score is defined as the inverse of ICER.

$$u_i(j,k) = \frac{E_j^{(i)} - E_k^{(i)}}{C_j - C_k} \tag{4}$$

$$U_k = \sum_i \sum_j u_i(j,k) \tag{5}$$

$$CE_j^{(i)} = \frac{C_j}{E_j^{(i)} - E_o^{(i)}} \tag{6}$$

In (4), the utility of the j-th plan compared to the k-th plan for the i-th contingency is denoted by $u_i(j,k)$. $E_j^{(i)}$ and $E_k^{(i)}$ are the effects of the j-th and k-th plans, respectively, when they are applied to the i-th contingency, defined as

the amount of load supplied. C_j and C_k are the annualized investment cost plus the annual operating cost of the j-th and k-th plans respectively. According to (4), a plan has higher utility if it supplies more power and has a lower annual cost, since a plan that can supply more power per additional dollar is considered to be more cost-effective. The total utility of the k-th plan U_k is calculated by summing over all the comparisons and contingencies as shown in (5). The average cost-effectiveness ratio for the j-th plan in the i-th contingency $CE_j^{(i)}$ is calculated as shown in (6), where $E_o^{(i)}$ is the active power supplied in that scenario without any additional generators. The utility function is used to build the pairwise comparison matrices for the AHP algorithm using the transformations shown below.

$$x_{jk} = 1 + 8\left(\frac{\frac{1}{P_j^{US}} - \frac{1}{P_k^{US}}}{\max P^{US} - \min P^{US}}\right) \tag{7}$$

$$a_{jk} = \begin{cases} x_{jk} & : x_{jk} \geq 1 \\ \frac{1}{x_{jk}} & : x_{jk} < 1 \\ 1 & : otherwise \end{cases} \tag{8}$$

$$y_{jk}^{(i)} = 1 + 8\left(\frac{\sum_l u_i(l,j) - \sum_l u_i(l,k)}{u_{max}^{(i)} - u_{min}^{(i)}}\right) \tag{9}$$

$$b_{jk}^{(i)} = \begin{cases} y_{jk}^{(i)} & : y_{jk}^{(i)} \geq 1 \\ \frac{1}{y_{jk}^{(i)}} & : y_{jk}^{(i)} < 1 \\ 1 & : otherwise \end{cases} \tag{10}$$

Contingencies are compared on the basis of severity, which is represented by the amount of unserved load. P_j^{US} and P_k^{US} are the total unserved load in the k-th and j-th contingencies, respectively. Therefore, criteria are assigned importance by (7)–(8), where $\max P^{US}$ and $\min P^{US}$ are the maximum and minimum unserved load across all contingencies, respectively. Similarly, option scores are calculated in (9)–(10), with $u_{max}^{(i)}$ and $u_{max}^{(i)}$ denoting the maximum and minimum utility among all plans for contingency i, respectively. A simple linear transformation is used to derive the matrices in each case.

III. Allocation and Sizing of PV and BESS

Transmission line outages reduce the number of available paths for power flow and may cause a shortfall in supply. If the connected generators are unable to supply the full load, the planning model adds appropriately sized solar PV arrays to connected nodes, along with a BESS as a backup source and storage for excess energy. The node with the highest unserved load across all the contingencies is selected for these resources. A disabled transmission line divides the grid into islands, which are groups of nodes with an existing path between each pair of nodes. In graph theory, such an island is called a connected component. To ensure that the demand is fully met, each island must have sufficient locally available generation capacity. Based on the results of AC OPF formulation described in Section II, the planning model allocates PV and BESS resources to each island.

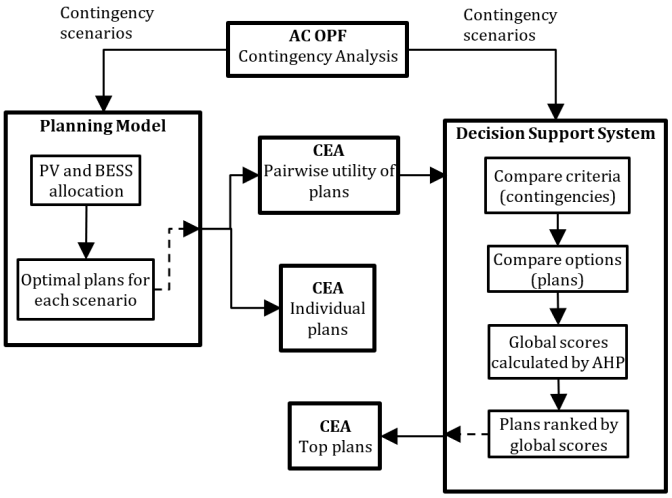

Fig. 2. Proposed planning framework for resilience enhancement.

TABLE I
PV PANEL PARAMETERS

PV panel	BP-Solar 3200
Rated power	200 W
Open-circuit voltage	30.8 V
Short-circuit current	8.7 A
Optimum voltage	24.5 V
Optimum current	8.16 A
Efficiency at STC	13%
Dimensions (L/W/D)	1680 × 837 × 50 mm
Cost per panel	$420
O&M cost	$15/kW

A. Photovoltaic Resources

A PV array equipped with a dc-ac inverter and a maximum power point tracking (MPPT) controller has a power output the depends on the solar irradiance and temperature. The PV array installed for island i is rated at $P_{pv\_r}^{(i)}$ with a derating factor of $f_{pv}^{(i)}$ to account for various factors such as shading and wiring losses. The actual power output of the array $P_{pv}^{(i)}$ depends on the on the solar insolation G and the temperature T. The solar radiation and temperature under standard test conditions are given by G_{STC} and T_{STC} respectively, while α_T is the temperature coefficient.

$$P_{pv}^{(i)} = f_{pv}^{(i)} P_{pv\_r}^{(i)} \frac{G}{G_{STC}}[1 + \alpha_T(T - T_{STC})] \tag{11}$$

$$f(G; a, b) = \frac{\Gamma(a+b)}{\Gamma(a)\Gamma(b)}\left(\frac{G}{G_{max}}\right)^{a-1}\left(1 - \frac{G}{G_{max}}\right)^{b-1} \tag{12}$$

$$P_{pv\_r}^{(i)} = n_{pv}^{(i)} P_{pv\_unit} \tag{13}$$

The expression in (11) gives the instantaneous PV power output for a given solar radiation and temperature. Since solar irradiance changes with time, the output power also varies, so a stochastic model is needed to account for the time-varying nature and suggest an appropriate value for G. As in many

TABLE II
LEAD-ACID BATTERY PARAMETERS

Battery	Hoppecke 6OPzS 600
Rated capacity	600 Ah
Rated voltage	2 V
Minimum SOC	35%
Round-tip efficiency	85%
Max. charge/discharge rate	0.5 A/Ah, 0.5 A/Ah
Max. charge/discharge current	100 A/75 A
Self-discharge rate	1%
Dimensions (L/W/D)	215 × 193 × 710 mm
Cost per cell	$150
O&M cost	$20/kAh

previous studies, the insolation is assumed to follow a beta probability distribution function [35] given by (12), where a and b are the shape parameters of the beta distribution and γ is the gamma function. Therefore, the allocated PV resources would have to be oversized in order to supply the demand. In (13), PV installation for island i is shown to be made up of $n_{pv}^{(i)}$ discrete units, each with rated power P_{pv_unit} . The full list of parameters of the PV panels used is provided in Table I.

B. Lead-Acid Battery

Since PV arrays alone cannot reliably supply power, some form of energy storage is needed to match supply with demand. Usually, lead-acid batteries are combined with PV arrays for this purpose. The battery can be charged during periods of surplus production and discharged when there is a deficit, so that the loads are always supplied. Allocation of batteries to each island is described by

$$Q_{bs}^{(i)} = n_{bs}^{(i)} Q_{bs\_unit} \tag{14}$$

where $Q_{bs}^{(i)}$ is the ampere-hour capacity of the BESS installed in island i, $n_{bs}^{(i)}$ is the number of cells in the battery, and Q_{bs_unit} is the rated ampere-hour capacity of each cell. The ampere-hour charge is used here since for batteries it is more convenient than energy or power. The BESS also includes an inverter and charge controller. The maximum depth of discharge and the efficiencies of the inverter and controller are considered in the model. Since PV arrays provide no power during the night, a robust sizing strategy is used to decide the BESS capacity so that it can take on the entire unserved load by itself. In this study, the battery is modeled as a dispatchable generator without internal dynamics of energy charge/discharge. Table II gives the details of the lead-acid battery cells used.

C. Annual Cost

The purpose of the planning model is the optimal sizing and allocation of the resources to enhance resilience and minimize total cost. This is formulated as an optimization problem with the total annual cost as the objective function and the various requirements enforced as constraints.

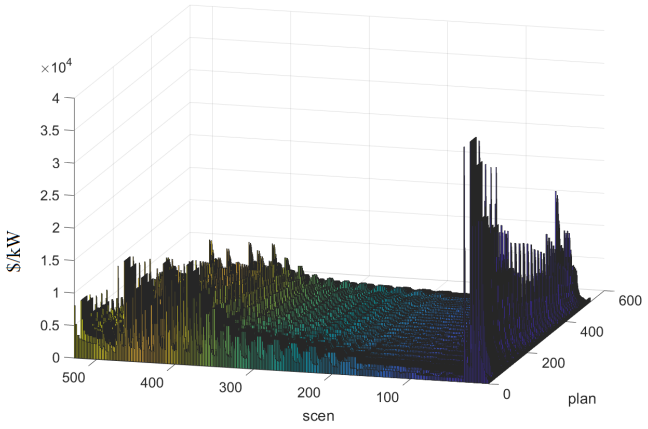

Fig. 3. Cost-effectiveness for all plans and scenarios.

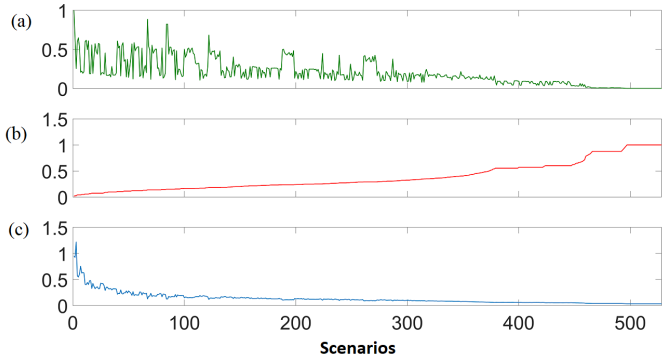

Fig. 4. Relationship between normalized (a) total unserved load, (b) cost, and (c) utility score.

$$\min_{n_{pv}^{(i)}, n_{bs}^{(i)}} f_{cr} \left(C_{pv} \sum_i n_{pv}^{(i)} + C_{bs} \sum_i n_{bs}^{(i)} \right) + C_{pv\_OM} \sum_i P_{pv\_r}^{(i)} + C_{bs\_OM} \sum_i Q_{bs}^{(i)} \tag{15}$$

$$f_{cr} = \frac{r(1+r)^L}{(1+r)^L - 1} \tag{16}$$

Total annualized cost is represented as expression in (15). The initial investment cost is found by multiplying the number of installed units by the cost per unit. C_{pv} and C_{bs} are the costs of each PV and BESS unit respectively, as specified in Tables I and II. The cost is annualized by multiplying it with the capital recovery factor f_{cr}, calculated as in (16), where r is the interest rate and L is the project lifetime. The annual operating and maintenance cost is calculated using the per unit capacity costs of PV and BESS, which are C_{pv_OM} and C_{bs_OM} respectively. Since resilience enhancement is the primary goal and normal operation is not a priority, fuel savings and tax credits are not included in the cost calculations, unlike in [26]. However, realistically a system planner would intend to use the PV generation and cheap electricity used to charge the BESS during off-peak hours to get added return on investment.

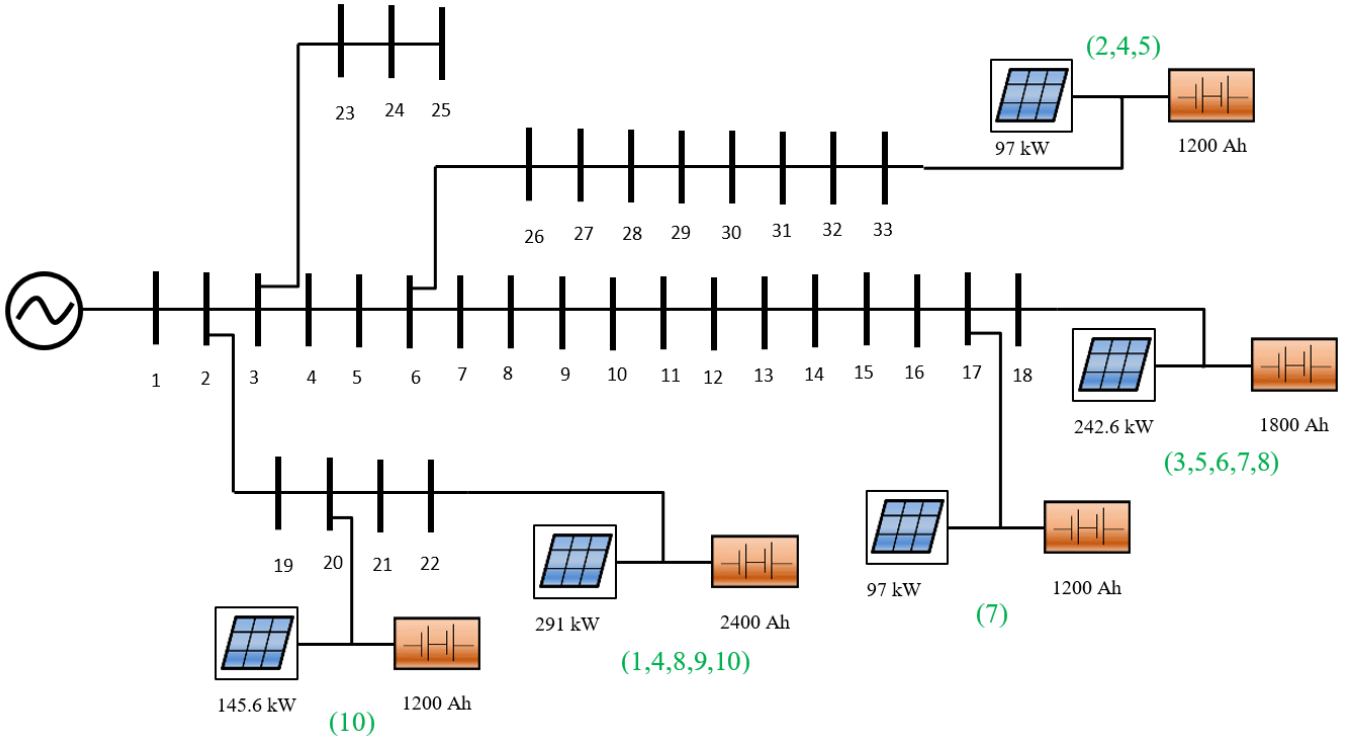

Fig. 5. The 33-bus distribution system with top 10 plans implemented, showing rated solar array power and battery capacity along with options.

These considerations would reduce the total annualized cost and provided a further incentive for generation expansion.

IV. Case Study

Radial power distribution systems are particularly vulnerable to line outages, since disruption of a single line may cut off multiple buses from power. The proposed planning method is tested on the standard IEEE 33-bus system, a 12.66 kV radial distribution system with total active and reactive power of 3.71 MW and 2.3 MVAR respectively [37]. Numerical solutions are obtained using CPLEX 12.8.0.0 optimization solver in MATLAB. All first- and second-order contingencies (one and two lines disabled, respectively) are simulated using the AC OPF model to yield the amount of load shed at each node, considering all loads as dispatchable. The SOCP model is run for 528 contingencies. In the planning model, mixed-integer linear programming (MILP) is used to solve the optimization problem of minimizing total annual cost for each contingency scenario. The numerical solution to the MILP problem gives the optimal plans for all scenarios, which are used as options in the AHP decision-making stage.

A. Evaluation of Recommended Plans

The cost-effectiveness of each option for all scenarios is evaluated using (6) and the result is shown in Fig. 3. Cost per unit power varies significantly among the plans, indicating the need for CEA even without considering the severity of the contingencies. Plans are generally the least cost-effective for the first few scenarios, where most of the buses are disconnected from the only generator bus (bus 1). These are the scenarios with the highest load shedding and require the most expensive plans. Comparison of the options on the basis of unserved load, cost and utility (normalized with respect to the maximum), demonstrated in Fig. 4, show that costlier plans supply more power but generally tend to be less cost-effective. This trend of diminishing returns means that the planner must consider the trade-off between performance and cost-effectiveness using the decision support system described in Section II. Since the utility score is based on the pairwise comparison of plans, Fig. 4 indicates that cheaper plans are generally preferable to expensive ones.

Plans recommended by AHP are based on comparative evaluations using the utility function defined in (4). All the options are ranked according to their global scores assigned by AHP. The options are not mutually exclusive and often overlapping. For example, if Plan A requires a 728-cell solar array and Plan B requires a 1213-cell solar array at the same bus, then implementing Plan B is equivalent to combining the two. The planner may choose to combine multiple options while staying within budget. Fig. 5 shows the result of implementing the first 10 plans recommended by AHP. The PV and BESS units are added preferentially to terminal buses, which are more vulnerable to load shedding due to being further away from the generation bus.

B. Coverage Level

The results shown in Figs. 3-5 have assumed that the planner intends to cover all of the unserved load with additional

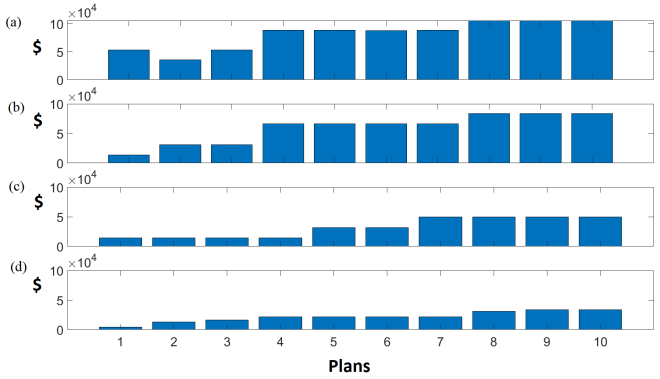

Fig. 6. Cost for the top 10 plans for (a) 100% (b) 99% (c) 95% and (d) 80% coverage.

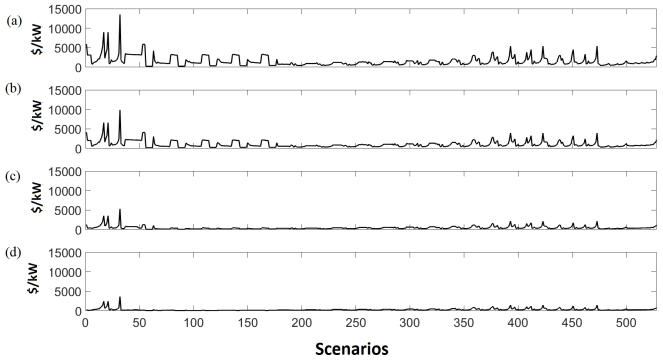

Fig. 7. Total cost-effectiveness for (a) 100% (b) 99% (c) 95% and (d) 80% coverage.

generation. In reality, all loads may not be equally important and there may be an upper limit on the investment cost due to budget constraints. Therefore, the effect of reducing the coverage of unserved load is also investigated in this case study. This is done by changing the constraints of the optimization problem in the planning model to require only partial compensation of the unserved load. For some contingency scenarios, the annualized cost of the optimal plan becomes zero, since the unserved load is too low to be considered for planning. These plans are considered trivial and ignored in the AHP stage. Fig. 6 compares the cost of the top 10 plans for different levels of coverage. Fig. 7 does the same thing for total cost-effectiveness, defined as the sum of $CE_j^{(i)}$ for all contingencies i, revealing a pattern similar to Fig. 3. The results show a significant reduction in total cost and cost per unit power as the coverage level is reduced from 100% to 80%. This is the same trend seen in Fig. 3 of more expensive plans not only costing more in total but also being more expensive per kW.

The average cost per kW of additional power capacity, calculated over all the plans and scenarios, is plotted for a broader range of coverage levels in Fig. 8. It shows conclusively that each unit of resilience enhancement becomes more expensive as larger proportions of loads are planned for. The increase in cost-per-unit is not linear but speeds up with higher coverage due to its dependence on higher order terms. Although a mathematical analysis of this relationship is beyond the scope of this paper, the results suggest that costs scale faster than a linear rate, which planners of large systems should be aware of. The coverage level is a matter of policy for the planner. In this study, all the loads are assumed to be dispatchable and equally weighted. A more detailed model could include weighted loads or partitioning the set into vital and non-vital loads. This would make some loads more expensive to cover, based on not just size but also location.

V. Conclusion

This paper presents a flexible and generalizable decision-making framework to enhance the resilience of a power system against transmission line outages while making the best use of financial investment. Contingencies are simulated by an AC OPF model and the results are used as input for the planning stage, where PV and BESS resources are optimally allocated to ensure that all loads are supplied at minimum cost. Since multiple contingencies are being considered and several plans are possible, AHP is used as a decision support system to choose between the available alternatives, which are assigned utility scores based on resilience and cost. The alternatives are ranked according to their cost-effectiveness and performance in various contingency scenarios with varying severity. A case study conducted on the 33-bus radial distribution system demonstrates the effectiveness of the framework as a decision support tool. Analysis of the results shows that decision-makers can reduce the cost per unit power by choosing cheaper generation expansion plans and allowing some load shedding to occur. The non-linear relationship between the cost per unit of additional power and total proportion of loads supplied is also demonstrated.

The proposed method offers significant flexibility and transparency for decision-makers. In this study, cost and resilience have been considered as the determining factors for the utility of alternative plans, but any number of factors may be included. Some simplifying assumptions have been made to ensure that the framework is applicable to any site, but the patterns and conclusions demonstrated in the case study

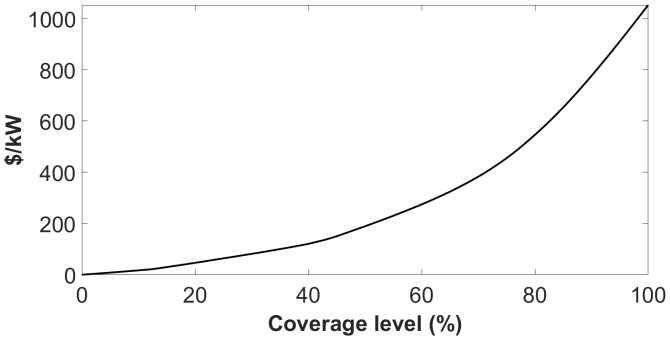

Fig. 8. Average cost-effectiveness for different levels of coverage, for 0% to 100%.

should hold regardless of the particular model parameters used. The utility function may be replaced by a different formula or an implicit system such as a learning algorithm. The set of scenarios may be expanded to include higher-order contingencies. Quantitative analysis reveals patterns that may help planners make a compromise between cost and resilience, perhaps through a secondary decision support system based on their own priorities. Since AHP only uses linear transformations, it may be scaled up to include more contingencies and allocation plans without requiring significantly greater computational power. The list of options in the case study of Section IV has been limited to the optimal plans for all scenarios, but the planning model may be expanded to generate any number of options. The framework developed in this paper helps decision-makers choose the best generation expansion strategy to limit cost and maximize resilience. This approach provides decision-makers with a tool for evaluating multiple contingency plans and building a resilient power system that can remain operational despite the occurrence of rare extreme events.

REFERENCES

[1] E. S. Blake and D. A. Zelinsky, Tropical Cyclone Report: Hurricane Harvey (AL092017), Miami, FL, May 2018

[2] J. P. Cangialosi, A. S. Latto, and R. Berg, Tropical Cyclone Report: Hurricane Irma (AL112017), Miami, FL, Jun. 2018.

[3] Y. Wang, C. Chen, J. Wang, and R. Baldick, "Research on Resilience of Power Systems under Natural Disasters - A Review," *IEEE Trans. Power Syst.*, vol. 31, no. 2. pp. 1604–1613, Mar. 2016.

[4] P. Hines, J. Apt, and S. Talukdar, "Trends in the history of large blackouts in the United States," in *2008 IEEE Power and Energy Society General Meeting - Conversion and Delivery of Electrical Energy in the 21st Century*, 2008, pp. 18.

[5] Z. Bie, Y. Lin, G. Li, and F. Li, "Battling the Extreme: A Study on the Power System Resilience," *Proc. IEEE*, vol. 105, no. 7, pp. 1253–1266, Jul. 2017.

[6] M. Panteli and P. Mancarella, "The Grid: Stronger, Bigger, Smarter?: Presenting a Conceptual Framework of Power System Resilience," *IEEE Power Energy Mag.*, vol. 13, no. 3, pp. 58–66, May 2015.

[7] C. Chen, J. Wang, and D. Ton, "Modernizing Distribution System Restoration to Achieve Grid Resiliency Against Extreme Weather Events: An Integrated Solution," *Proc. IEEE*, vol. 105, no. 7, pp. 1267–1288, Jul. 2017.

[8] M. Panteli, C. Pickering, S. Wilkinson, R. Dawson, and P. Mancarella, "Power System Resilience to Extreme Weather: Fragility Modeling, Probabilistic Impact Assessment, and Adaptation Measures," *IEEE Trans. Power Syst.*, vol. 32, no. 5, pp. 3747–3757, Sep. 2017.

[9] G. Li et al., "Risk Analysis for Distribution Systems in the Northeast U.S. Under Wind Storms," *IEEE Trans. Power Syst.*, vol. 29, no. 2, pp. 889–898, Mar. 2014.

[10] S. Mukherjee, R. Nateghi, and M. Hastak, "A multi-hazard approach to assess severe weather-induced major power outage risks in the U.S.," *Reliab. Eng. Syst. Saf.*, vol. 175, pp. 283–305, Jul. 2018.

[11] T. Amraee and H. Saberi, "Controlled islanding using transmission switching and load shedding for enhancing power grid resilience," *Int. J. Electr. Power Energy Syst.*, vol. 91, pp. 135–143, 2017.

[12] T. Ding, Y. Lin, Z. Bie, and C. Chen, "A resilient microgrid formation strategy for load restoration considering master-slave distributed generators and topology reconfiguration," *Appl. Energy*, vol. 199, pp. 205–216, 2017.

[13] H. Farzin, M. Fotuhi-Firuzabad, and M. Moeini-Aghtaie, "Enhancing Power System Resilience Through Hierarchical Outage Management in Multi-Microgrids," *IEEE Trans. Smart Grid*, vol. 7, no. 6, pp. 2869–2879, Nov. 2016.

[14] S. Chanda and A. K. Srivastava, "Defining and Enabling Resiliency of Electric Distribution Systems with Multiple Microgrids," *IEEE Trans. Smart Grid*, vol. 7, no. 6, pp. 2859–2868, Nov. 2016.

[15] A. Dubey and S. Poudel, "A robust approach to restoring critical loads in a resilient power distribution system," in *IEEE Power and Energy Society General Meeting*, 2017, pp. 15.

[16] Y. Fang and G. Sansavini, ''Optimizing power system investments and resilience against attacks," *Reliab. Eng. Syst. Saf.*, vol. 159, pp. 161–173, Mar. 2017.

[17] C. Shao, M. Shahidehpour, X. Wang, X. Wang, and B. Wang, "Integrated Planning of Electricity and Natural Gas Transportation Systems for Enhancing the Power Grid Resilience," *IEEE Trans. Power Syst.*, vol. 32, no. 6, pp. 4418–4429, Nov. 2017.

[18] K. Lai and M. S. Illindala, "Graph Theory Based Shipboard Power System Expansion Strategy for Enhanced Resilience," *IEEE Trans. Ind. Appl.*, vol. 54, no. 6, pp. 5691–5699, 2018.

[19] R. Arghandeh et al., "The Local Team: Leveraging Distributed Resources to Improve Resilience," *IEEE Power Energy Mag.*, vol. 12, no. 5, pp. 76–83, Sep. 2014.

[20] W. D. Kellogg, M. H. Nehrir, G. Venkataramanan, and V. Gerez, "Generation unit sizing and cost analysis for stand-alone wind, photovoltaic, and hybrid wind/PV systems," *IEEE Trans. Energy Convers.*, vol. 13, no. 1, pp. 70–75, Mar. 1998.

[21] W. Kellogg, M. H. Nehrir, G. Venkataramanan, and V. Gerez, "Optimal unit sizing for a hybrid wind/photovoltaic generating system," *Electr. Power Syst. Res.*, vol. 39, no. 1, pp. 35–38, Oct. 1996.

[22] R. Chedid and S. Rahman, "Unit sizing and control of hybrid wind-solar power systems," *IEEE Trans. Energy Convers.*, vol. 12, no. 1, pp. 79–85, Mar. 1997.

[23] Lin Xu, Xinbo Ruan, Chengxiong Mao, Buhan Zhang, and Yi Luo, "An Improved Optimal Sizing Method for Wind-Solar-Battery Hybrid Power System," *IEEE Trans. Sustain. Energy*, vol. 4, no. 3, pp. 774–785, Jul. 2013.

[24] G. B. Shrestha and L. Goel, "A study on optimal sizing of stand-alone photovoltaic stations," *IEEE Trans. Energy Convers.*, vol. 13, no. 4, pp. 373–378, Dec. 1998.

[25] D. L. Talavera, F. J. Muñoz-Rodriguez, G. Jimenez-Castillo, and C. Rus-Casas, "A new approach to sizing the photovoltaic generator in self-consumption systems based on costcompetitiveness, maximizing direct self-consumption," *Renew. Energy*, vol. 130, pp. 1021–1035, Jan. 2019.

[26] C. Yuan, M. S. Illindala, and A. S. Khalsa, "Co-Optimization Scheme for Distributed Energy Resource Planning in Community Microgrids," *IEEE Trans. Sustain. Energy*, vol. 8, no. 4, pp. 1351–1360, Oct. 2017.

[27] M. H. Nehrir et al., "A review of hybrid renewable/alternative energy systems for electric power generation: Configurations, control, and applications," *IEEE Transactions on Sustainable Energy*, vol. 2, no. 4. pp. 392–403, Oct-2011.

[28] P. Denholm and R. M. Margolis, ''Evaluating the limits of solar photovoltaics (PV) in electric power systems utilizing energy storage and other enabling technologies," *Energy Policy*, vol. 35, no. 9, pp. 4424–4433, Sep. 2007.

[29] D. Álvaro, R. Arranz, and J. A. Aguado, "Sizing and operation of hybrid energy storage systems to perform ramp-rate control in PV power plants," *Int. J. Electr. Power Energy Syst.*, vol. 107, pp. 589–596, 2019.

[30] R. Domínguez, A. J. Conejo, and M. Carrión, Toward fully renewable electric energy systems, *IEEE Trans. Power Syst.*, vol. 30, no. 1, pp. 316326, Jan. 2015.

[31] A. Monticelli, M. V. F. Pereira, and S. Granville, "Security-Constrained Optimal Power Flow with Post-Contingency Corrective Rescheduling," *IEEE Trans. Power Syst.*, vol. 2, no. 1, pp. 175–180, 1987.

[32] X. Wu, A. J. Conejo, and N. Amjady, "Robust security constrained ACOPF via conic programming: Identifying the worst contingencies" *IEEE Trans. Power Syst.*, vol. 33, no. 6, pp. 5884–5891, Nov. 2018.

[33] R. A. Jabr, "Radial Distribution Load Flow Using Conic Programming," *IEEE Trans. Power Syst.*, vol. 21, no. 3, pp. 1458–1459, Aug. 2006.

[34] T. L. Saaty, "How to make a decision: The analytic hierarchy process," *Eur. J. Oper. Res.*, vol. 48, no. 1, pp. 9–26, Sep. 1990.

[35] Y. M. Atwa, E. F. El-Saadany, M. M. A. Salama, and R. Seethapathy, "Optimal renewable resources mix for distribution system energy loss minimization," *IEEE Trans. Power Syst.*, vol. 25, no. 1, pp. 360–370, 2010.

[36] A. J. Conejo et al., "Investment in Generation and Transmission Facilities," in *Investment in Electricity Generation and Transmission*, Cham: Springer International Publishing, 2016, pp. 1–19.

[37] M. E. Baran and F. F. Wu, "Network reconfiguration in distribution systems for loss reduction and load balancing," *IEEE Trans. Power Deliv.*, vol. 4, no. 2, pp. 1401–1407, Apr. 1989.